Published in final edited form as:
Health Phys. 2010 February ; 98(2): 301–308. doi:10.1097/HP.0b013e3181b0c045.

Ex Vivo Analysis of Irradiated Finger Nails: Chemical Yields and Properties of Radiation-Induced and Mechanically-Induced Radicals

Paul J. Black[*] and **Steven G. Swarts**[‡]

[*]Department of Biochemistry/Biophysics University of Rochester, Rochester, New York 14642

[‡]Department of Radiation Oncology, University of Rochester, Rochester, New York 14642

Abstract

A qualitative and quantitative analysis of the radicals underlying the radiation induced signal (RIS) in finger nails was conducted in an attempt to identify properties of these radicals that could be used for biodosimetry purposes. A qualitative analysis of RIS showed the presence of at least three components, two of which were observed at low doses (<50 gray) and the third required higher doses (>500 gray). The low dose signal, obtained by reconstruction, consists of a 10 gauss singlet at g = 2.0053 and an 18 gauss doublet centered at g = 2.0044. Based on the initial slope of the dose response curve, the chemical (radical) yields of the radicals giving rise to the singlet and doublet were 327 (±113) and 122 (±9) nmol J^{-1} (S.E.), respectively. At doses below 50 gray, the singlet signal is the dominant component. Above this dose range, the signal intensity of the singlet rapidly dose saturates. At doses < 50 gray, there is a small contribution of the doublet signal that increases in its proportion of the RIS as dose increases. A third component was revealed at high dose with a spectral extent of ~100 gauss and displayed peaks due to g anisotropy at g = 2.056, 2.026, and 1.996. The total radical yield calculated from the initial slope of the dose response curve averaged 458 ± (116) nmol J^{-1} (S.E.) in irradiated nail clipping obtained from six volunteers. Such high yields indicate that nails are a strong candidate for biodosimetry at low doses. In a comparison of relative stabilities of the radicals underlying the singlet and doublet signals, the stability of the doublet signal is more sensitive to the moisture content of the nail than the singlet. This differential in radical stabilities could provide a method for removing the doublet signal under controlled exposures to high humidities (>70% relative humidity). The decay of the singlet signal in RIS varies with exposure of a nail clipping to differing ambient humidities. However, long exposures (> 6 hr) to relative humidities of 72-94% results in singlet intensities that approach 7.0 ± (3.2)% (S.D.) of the original intensities in an irradiated nail. This result suggests the existence of a subpopulation of radicals underlying the singlet signal that are relatively insensitive to decay under exposure of nails to even high humidities. Therefore, exposures of an irradiated nail clipping under controlled humidities may provide a method for estimating the exposure dose of the nail that is based on the intensity of the signal of the humidity insensitive radical population underlying the singlet signal.

Keywords

ionizing radiation; radiation damage; biodosimetry; electron paramagnetic spectrometry

Corresponding Author: Steven G. Swarts, Ph.D. Department of Radiation Oncology, University of Rochester, 601 Elmwood Avenue, Box 647, Rochester, New York 14642, FAX: (585) 275-1531, Phone: (585) 275-0119, Steven_Swarts@urmc.rochester.edu.

Introduction

Changes due to ionizing radiation (IR) in fingernails have the potential to serve as the basis of a biodosimetric method in humans exposed to ionizing radiation. This was recognized two decades ago by Symons and colleagues (Symons et al. 1995). In recent years, attempts to tap this potential have been undertaken by several research groups (Reyes et al. 2008; Romanyukha et al. 2007; Trompier et al. 2007). The work of Symons and co-workers (Symons et al. 1995; Symons 1997) provided some suggestions as to the reaction mechanisms of IR-induced radicals and the chemical structure of the main radical species trapped in the fingernail matrix. Because the main component of fingernail is α-keratin, it is assumed that radicals are formed by one-electron oxidation or one-electron reduction of this protein. It has been suggested that at ambient temperatures the reaction of electron loss (e.g. "holes") and electron gain centers on α-keratin will result in the formation of primary radicals, for example peptide backbone amide radical cations and cystine disulfide radical anions, respectively. However, neither of these radicals are observed in the nail spectra. Instead, the singlet that is observed is due to unknown secondary radical(s).

One problem that has been encountered in the ex vivo analysis of the RIS in nails is the formation of a mechanically-induced signal (MIS) in the nail (Chandra and Symons 1987; Romanyukha et al. 2007; Romanyukha et al. this issue; Trompier et al. 2007; Wilcox et al. this issue). This MIS is due to α-keratin radicals that are likely formed along the shear edge of the nail when the nail is clipped. The MIS contains spectral features that overlap with the RIS spectrum. These features often have intensities that can easily overwhelm the RIS formed at doses below 10 gray (Gy). It has been suggested that the MIS is due predominantly to the presence of sulfuranyl radicals formed as a consequence of reaction of mechanically-induced radicals with neighboring cystine bridges in the α-keratin fibers (Chandra and Symons 1987; Symons et al. 1995). In more current work there is evidence that other radicals also contribute to the MIS. The contribution of these other radicals to the overall spectrum depends on time elapsed from nail clipping and perhaps on the moisture content of the nail (Reyes et al. 2008).

In order to properly quantify the RIS in irradiated nails it is necessary to develop strategies to preferentially remove the interfering MIS from the nail. There are a number of approaches that have been proposed and explored to accomplish this (Reyes et al. 2008; Romanyukha et al. 2007; Romanyukha et al. this issue; Trompier et al. 2007; Wilcox et al. this issue). It is important to characterize the radical species underlying the MIS and RIS in addition to their radical reaction processes. Radical stabilities under a variety of nail treatments and ambient conditions are important for obtaining reliable dose estimates based on RIS measurements. The goal of this work is to provide a qualitative analysis of the RIS radicals, their spectra and reactivities in order to better develop methods for removing the MIS interference from the spectra of irradiated nails and improving the accuracy of the RIS measurements, especially with respect to estimating the intensity of the RIS signal at the time of radiation exposure.

Materials and Methods

Sample Preparation

Fingernail clippings were obtained from adult volunteers according to an IRB approved University of Rochester protocol, URCC U3607. Clippings weighing 6-15 mg were collected as single pieces and used within 10 min after harvesting (for MIS studies). For RIS studies the nail clippings were used either immediately after harvesting or stored at 253 K in a sealed container up to 48 hr before use. Prior to irradiation, nail clippings were soaked in water for 10 min and air dried for 20 min to remove the MIS signal and to return the nail to a

pre-cut state (Reyes et al. 2008). For RIS and most MIS studies, whole nail clippings were used. For studies of humidity dependent changes in MIS nail clippings were cut into smaller 2×2 mm (10-12) pieces to maximize the MIS.

Sample Irradiation

For the EPR analysis, the nails were gamma-irradiated (Model 109 ^{60}Co irradiator, JL Sheppard and Associates) or x-irrradiated using a Varian/Eimac OEG-76H tungsten target tube operated at 70 kV, 20 mA. Dosimetry for both radiation sources is calculated using radiochromic film dosimetry methods. The x-ray source was used in the dose-response and RIS decay kinetics studies. A dose rate of 8 Gy min^{-1} was used for doses of 10-200 Gy; a dose rate of 1 kGy min^{-1} was used for doses of 500-1,000 Gy., The ^{60}Co source was used for the water soak treatment studies of RIS at a dose rate of 8.3 Gy min^{-1}. Following irradiation, the nails were analyzed at 295 K under either ambient humidity or controlled humidities using a hydrated air stream (one-stage bubbler).

EPR Analysis

Radiation-induced protein radicals in the nail samples were analyzed at 295 K using an X-band (9.37 GHz) IBM (Brüker) ER 200D-SRC EPR spectrometer equipped with a Hewlett-Packard 2328 microwave frequency counter and a Varian dual cavity. First derivative spectra were acquired at incident microwave powers of 1.99 mW and modulation amplitudes of 3.2-5 gauss (G). Single or paired nail samples were placed vertically along the long axis in the cavity within a finger dewar (5 mm inner diameter). The nails were positioned so that the curvature of the clipping was aligned within the plane of the B field of the incident microwave radiation. For some MIS studies, 2×2 mm nail clippings (10-12) were loaded into 3 mm EPR tubes for EPR analysis. The mass of the nail clippings was kept at 12±1 mg for the MIS studies. In studies of humidity-dependent changes in the MIS or RIS, stream of dry or humidified air was directed into the dewar. The relative humidities (r.h.) were measured using a digital hygrometer placed in-line with the dry or humidified air stream.

Sample Analysis

Using the Varian dual cavity, we were able to place and measure qualitative or quantitative internal standards within the same resonator as the nail samples without the interference of overlapping standard and sample spectra. Qualitative analysis and deconvolution of spectra was done in reference to Fremy salt ($g = 2.0056$, $a_N = 13.09$ G). Quantitative analysis of the RIS and MIS spectra were done either by: 1) measuring peak-to-peak or peak-to-baseline spectral intensities, or 2) determining the number of spins (double integral of the spectra) within all or select regions of the spectra. The free radical concentration was calculated relative to a $CuCl_2 \cdot 2H_2O$ reference standard (36 μg = 1.27×10^{17} spins). In all nail samples used for RIS studies, spectra were acquired prior to irradiation to obtain the background signal, which was subtracted from any subsequent RIS spectra obtained following irradiation of the nail. For the deconvolution studies, the basis spectrum for the RIS singlet was produced by irradiating a nail (soaked in water for 10 min, dried for 20 min prior to irradiation) to 50 Gy and then exposing the nail to 92% r,h. for 4 hr to remove a small broader feature. The basis spectrum for the MIS singlet was produced by exposing nail clippings (2×2 mm, 10 pieces) to 74% for 24 hr. For the study of RIS decay kinetics, one- or two-phase exponential or linear fits to the decay data were performed using GraphPad Prism version 5.0a for Windows, GraphPad Software, San Diego California USA, www.graphpad.com). A two-phase exponential function ($(Y = \text{Plateau} + A \times \exp(-K_{Fast}X) + B \times \exp(-K_{Slow}X)$ where $A = (Y0\text{-Plateau}) \times \text{PercentFast} \times 0.01$ and $B = (Y0\text{-Plateau})(100\text{-PercentFast}) \times 0.01$) was used to fit in the analysis of total RIS given that two radical components contributed to these spectra. A one-phase exponential function ($Y = (Y0$ -

Plateau) × exp(-KX) + Plateau) was used to fit to the decay of the singlet, whereas a linear function was used to fit the doublet data.

Results and Discussion

The ex vivo analysis of the RIS in finger (or toe) nails by the EPR technique is complicated by the presence of an MIS that is formed presumably at the shear edge of the nail clipping following harvesting. The difficulty in performing a measurement of the RIS is the overlap and often comparable intensities in the spectral features between the RIS and MIS in the overall signal of an irradiated nail clipping, as has been shown in several recent studies (Reyes et al. 2008; Romanyukha et al. 2007; Romanyukha et al. this issue; Trompier et al. 2007; Wilcox et al. this issue). For example, the singlet feature seen in the both the RIS and MIS is commonly observed in both sources of nail signal and is the most stable signal. However, the qualitative features of the RIS and MIS change as a function of dose (RIS), as shown in Fig. 1, and time from harvesting (MIS) especially when exposed to various ambient conditions such as humidity (MIS), as shown in Fig. 2. Another complication is the presence of at least three distinct spectral features that can be found in both the RIS and MIS spectra. This is illustrated in Figs. 3 and 4, which show comparable total spectra for RIS in an irradiated nail (1,000 Gy) and MIS in an unirradiated nail, respectively. These spectra can be deconvoluted into a singlet (Figs. 3B and 4B) and doublet (Figs. 3C and 4C). A third spectral component can be seen at g = 2.056 and g = 2.022. These MIS spectral features have been observed in other recent studies (Reyes et al. 2008; Romanyukha et al. this issue; Wilcox et al. this issue). However, the doublet and third spectral component have not been well characterized in RIS. Therefore, to accurately measure the RIS component in an irradiated nail, strategies must be devised to preferentially remove the overlapping MIS interference without adversely affecting the RIS.

Several methods for removing MIS from nail clippings have been tested that exploit the sensitivity of the MIS to accelerated decay as a consequence of various physical treatments, such as soaking nails in solvents or aqueous solutions (Reyes et al. 2008; Romanyukha et al. 2007; Trompier et al. 2007). Spectral deconvolution methods are being examined that take advantage of time evolution and power saturation differences between the three spectral components in MIS (Wilcox et al. this issue). Both approaches show good potential for eliminating MIS from irradiated nail spectra and are described in the literature. However, there are some concerns when using physical methods (i.e. water soak) methods or spectral deconvolution techniques for removing MIS. It is likely that the water soak method is acting to enhance the reactivity of the radicals underlying the MIS through increased translational action of the nail matrix and radical mobilities. Because the radicals underlying the MIS are believed to reside at the shear edge of the nail clipping, a short 10 min water soak is expected to preferentially reduce the stability of the MIS radicals at the surface of the nail. Yet, the soak can also affect the stability of the radicals underlying the RIS, depending on the extent of water penetration into the nail. Fig. 5 shows the decrease in the RIS as a function of soak time of irradiated nail clippings where a 20% decrease in signal is observed after a 10 min soak time. Regarding spectral deconvolution approaches, there are dose dependent qualitative and quantitative changes in the RIS as shown in Fig. 1 that must be considered. Both the stability and dose dependent changes in RIS need further examination in order to fully develop methods or removing the interference of MIS from irradiated nails.

In an attempt to gain additional insights into the dose dependencies of the RIS and examine the relative stabilities of the radicals underlying RIS we have used high dose studies of nails to achieve greater signal quality to better characterize the RIS radicals. Dose response studies were used to examine the dose dependent behavior of the underlying RIS radicals. At a 10 Gy dose only one feature of the RIS stands out, a singlet at 2.0053 with a peak-peak

width of 10 G. Increasing the dose causes the singlet to broaden. This becomes apparent at 20 Gy. Above 500 Gy a broad signal with peaks at g = 2.056, 2.026, and 1.996 becomes prominent. This signal, which has a spectral width of ~100 G, is attributed to either a perthiyl (Fig. 6A) or sulfuranyl (Fig. 6B) radical (Becker et al. 1988; Chandra and Symons 1987). The broader components of the RIS are not visible at low dose, but it is believed that they are still present but not readily detectable due to large line widths. The sharpest peak of the 100 G wide signal has a width around 30 G; in order to obtain a signal-to-noise comparable to the 10 G singlet, a factor of ~ 10× higher $(30/10)^2$ radical concentration would be needed. This is an important consideration when interpreting the free radical composition and the dose response curves.

Radical concentration was determined for only the center components of the RIS. A 50 G span of the center components was double integrated and compared to a standard of $CuCl_2 \cdot 2H_2O$ containing 1.27×10^{17} spins. Irradiation and measurements were conducted under temperatures of 294-296 K and 50-55% r.h. A typical dose-response is shown in Fig. 7 (square). The dose response curves were fit at doses between 0-200 Gy to the well-known dose response Equation (1) (Snipes and Horan 1967).

$$C = C_\infty(1 - \exp(-kD)) \quad \text{(Eq. 1)}$$

Due to radical destruction, governed by k, the radical concentration C dose saturates at a level C_∞ as dose, D, approaches infinity. As the dose increases, the curve departs from linearity due to radical destruction as a consequence of track-track overlap. The variable k is a measure of this destruction cross section. At zero dose, $C = C_\infty kD$ and $C_\infty = G\ k^{-1}$, therefore C = GD and the slope is dC/dD = G(fr), where G(fr) is.a measure of the chemical yield of free radicals.

Using the above analysis, the chemical yields of radicals giving rise to the center component are given in Fig. 8, representing data from six different people. The average chemical yield (e.g. G-value) was calculated to be 458 nmol J^{-1}, with a standard deviation (S.D.) of 116 nmol J^{-1}. The chemical yields that we have measured in nails for irradiations carried out at room temperature is only achievable if a material is highly efficient at trapping radicals. For example, DNA is considered to be an extremely efficient radical trap with a chemical yield at 4 K of approximately 600 nmol J^{-1} (Debije and Bernhard 2000). This indicates that the fingernail matrix, with a chemical yields ranging from 324-605 nmol J^{-1}, is a good radical trap at 295 K and, thereby, a strong candidate for biodosimetry at low doses under conditions that are relevant for estimating radiation dose in humans.

The characteristics that we observed for the 10 G singlet at g = 2.0053 agree well with those reported previously (Reyes et al. 2008; Romanyukha et al. 2007; Romanyukha et al. this issue; Symons et al. 1995; Wilcox et al. this issue). Symons et al. (1995) suggested that the singlet found in RIS may be due to amide radicals randomly localized on the peptide backbone. Another possible assignment of the RIS and MIS singlet is a cysteine sulphonyl radical, $CysSO_2\bullet$. This radical has been shown to also give an isotropic singlet with a g-value of 2.0055 and a 10 G linewidth in frozen LiCl glasses (Razskazovskii and Sevilla 1996). However, of the two assignments the peptide-backbone amide radical may more readily explain the rapid dose saturation in yields observed for the singlet (Fig. 7). It has been suggested that electrons formed in the radiolysis of proteins may migrate along the peptide backbone (Symons et al. 1995; Symons 1997). If so, then there is a good likelihood that these electrons could react with and eliminate amide radicals on the peptide backbone. For either assignment, the similarity in singlet spectra in the RIS and MIS and the power

saturation behaviors (Fig. 9) of these two signals would suggest that the same radical is present in the RIS and MIS.

Our dose response data helps add to this information by showing that there must be at least two other radical species giving rise to the RIS. One of these radical species must give a signal somewhat broader than the 10 G wide singlet so that, as dose is increased, an apparent broadening of the singlet occurs. A better view of this underlying spectrum was obtained by subtracting a basis spectrum for the singlet in Fig. 3B from the 1,000 Gy spectrum in Fig. 3A. The resulting doublet spectrum, Fig. 3C, is centered at g = 2.0044 and has a splitting of 18.7 G. This doublet fits the spectral characteristics expected for a carbon centered radical produced by the net loss of H from the α-carbons of the polypeptide backbone that are bonded to residues R = H or R = CH_2R' (Fig. 10). This assignment is based on evidence obtained from studies of small peptides with R = H or R = CH_2R' giving rise to α-carbon (peptide backbone) radicals that are characterized by an isotropic doublet with a splitting of 18-19 G (Sevilla et al.1979). This radical has been shown to be common in peptides and proteins irradiated in aqueous, frozen aqueous and solid state (e.g. powder) models systems (Garrison 1987). As suggested above, the similarity in these two spectral components in both the RIS and MIS argues that the underlying radicals responsible for the RIS and MIS are similar and differ only in their relative proportions as a consequence of the mechanism of formation of the RIS and MIS.

From spectral deconvolutions performed on each of the total RIS spectrum shown in Fig. 1, we were able to calculate the number spins for the singlet and doublet spectra at each dose between 0-1,000 Gy. From a plot of the number of spins as a function of dose (Fig. 7) it is found that the singlet (circle) begins to dose saturate above 30 Gy and essentially plateaus above 200 Gy. In contrast, the doublet signal (triangle) increases linearly with dose up to 1,000 Gy. Fitting the dose response data to Equation 1 we were able to calculate chemical yields (and standard errors, S.E.) of 327 (±113) and 122 (±9) nmol J^{-1} for the radicals underlying the singlet and doublet signals.

There is evidence to show that the decay rate of the RIS is influenced by the ambient humidity. However, the decay behavior does not show a simple dependence on relative humidity. The double integral analysis of the RIS singlet under 72% and 94% relative humidity conditions reveal that the signal follows a two-phase exponential decay. A typical decay curve is given in Fig. 11. The shape of the decay curve was consistent across many different individuals' nails, but the decay kinetics varied significantly. From the two-phase exponential fit of each decay curve, a fast half-life and slow half-life was calculated. The fast phase half-life values ranged from 1.33 min to 31.46 min with a standard deviation of 10.17 min. The slow phase half-life exhibited a much larger range and variance. This parameter ranged from 72.6 min to 284 min with an average of 105 min and a relative standard deviation (RSD) of 84%. The differences in the slow phase decay rates did not correlate well with the mass of the nail clipping. Even so, in all decay studies the percentage of the initial number of spins (at 10 min post-irradiation) in the RIS after long exposures to controlled humidities (> 6 hr) averaged to 7.0 ± 3.2 (1 S.D.). This average signal does not include the background signal, also noted as BKS (Reyes et al. 2008; Romanyukha et al. this issue), that can sometimes remain in a nail sample because it has either been eliminated by the pre-irradiation water-soak or subtracted from the RIS spectrum during the spectral analysis process. From the plot of the decay data for the singlet and doublet signals in a nail clipping as a function of decay time in Fig. 11, the fast and slow phase decay in our two-component fit of the total RIS spectral data approximate well the decay of the doublet and singlet signals, respectively. Furthermore, the decay rates at 94% relative humidity were not generally faster than those at 72%. However, the decay rates were slower at humidity levels that are typical for air conditioned buildings (ca. 45-55% r.h.). Under these conditions the

half-lives for the slow phase increase to an average of 2.4 days but result in a decrease in variability in the half-times (RSD = 43%) as compared to the data taken at 72% and 94% r.h. Therefore, consideration must be given to the exposure times and ambient relative humidity following an exposure event in order to extrapolate the measured RIS intensity to the initial intensity at the time of an exposure.

An interesting observation in our radical decay studies was the differential decay rates between at least two radical species underlying the RIS. In Fig. 11 it can be seen from nails irradiated to 1,000 Gy and exposed to 72% r.h. that there is a change from a mixture of the doublet (from the peptide backbone radical) and a singlet at g = 2.0053 to only the singlet. These results suggest that exposing a nail post-irradiation to controlled humidities can be used to remove the doublet signal from the RIS while controlling the decay of the singlet, thus providing a potential method for back extrapolating the singlet signal intensity (or integrated area) to pre-exposure levels.

Conclusion

EPR measurements of IR-induced signals in finger nails shows potential as a radiation biodosimeter. The nail acts as a good radical trap, with a yield > 300 nmol J^{-1} for just those radicals giving rise to the central singlet component that would be key to EPR dosimetry. The evidence from the work presented here suggests a common set of three radical populations underlying the RIS and MIS spectra. The contribution of these radical populations to the RIS and MIS are dependent on mechanism (i.e. radiolysis of protein for RIS and homolytic bond cleavage in nail proteins due to mechanical shearing of the nail during harvesting), time from harvesting or irradiation, moisture content as determined from exposure to water or ambient humidity, and dose (RIS). Other radicals may be present in the MIS and RIS that are not observable due to large line widths. For example, in the spectrum of the cysteine thiyl radical (which could be formed in irradiated nails based on its occurrence in studies of irradiated proteins) the g-parallel line extends over 400 G (Kolberg et al. 2002). Therefore, the qualitative and quantitative analyses of the MIS and RIS presented here may not include all possible radicals but are believed to include the major radicals underlying the MIS and RIS.

At doses below 50 Gy the singlet signal is dominant in the total RIS spectrum. Above this dose range, the signal intensity of the singlet rapidly dose saturates. At doses < 50 Gy, there is a small contribution of the doublet signal to the RIS that increases in its proportion of the RIS as dose increases. However, the stability of the doublet signal is more sensitive to the moisture content of the nail than the singlet, thereby providing a method for removing the doublet signal under controlled exposures to high humidities (>70% r.h.). The decay of the singlet signal in RIS varies with exposure of a nail clipping to differing ambient humidities. However, long exposures (> 6 hr) to r.h. of 72-94% results in singlet intensities that approach a mean (± 1 S.D.) of 7.0% (±3.2) of the original intensities in an irradiated nail. This result suggests the existence of a subpopulation of radicals underlying the singlet signal that are relatively insensitive to decay under exposures of the nail to even high humidities. Therefore, exposures of an irradiated nail clipping under controlled humidities may provide a method for estimating the exposure dose of the nail that is based on the intensity of the signal of the humidity insensitive radical population underlying the singlet signal. How this intensity of this insensitive subpopulation relates to the dose of the nail clipping remains to be tested.

Acknowledgments

This research was funded through a pilot grant sponsored by the University of Rochester CMCR under NIAID contract U19 AI067733.

The authors wish to thank Dr. William Bernhard for his invaluable assistance in experimental design, data analysis, and critique of this written work. Concept work for the finger nail biodosimeter was supported by Syracuse Research Corporation with help from Drs. Tony Gray and David Knaebel.

References

Becker D, Swarts S, Champagne M, Sevilla MD. An electron spin resonance investigation of the reactions of glutathione, cysteine and penicillamine thiyl radicals – competitive formation of RSO•, R•, RSSR(-•), and RSS•. Int J Radiat Biol. 1988; 53:767–786.

Chandra H, Symons MC. Sulfur radicals formed by cutting alpha-keratin. Nature. 1987; 328:833–834. [PubMed: 2442616]

Debije MG, Bernhard WA. Electron and hole transfer induced by thermal annealing of crystalline DNA x-irradiated at 4K. J Phys Chem B. 2000; 104:7845–7851.

Garrison WM. Reaction mechanisms in the radioloysis of peptides, polypeptides, and proteins. Chem Rev. 1987; 87:381–398.

Horan PK, Snipes W. The temperature dependence of radiation-induced free-radical destruction. Int J Radiat Biol. 1971; 19:37–43.

Kolberg M, Bleifuss G, Graslünd A, Sjöberg B-M, Lubitz W, Lendzian F, Lassman G. Protin thiyl radicals directly observed by EPR spectroscopy. Arch Biochem Biophys. 2002; 403:141–144. [PubMed: 12061811]

Razskazovskii Y, Sevilla MD. Reactions of sulphonyl peroxyl radicals with DNA and its components: hydrogen abstraction from the sugar backbone versus addition to pyrimidine double bonds. Int J Radiat Biol. 1996; 69:75–87. [PubMed: 8601758]

Reyes RA, Romanyukha A, Trompier F, Mitchell CA, Clairand I, De T, Benevides LA, Swartz HM. Electron paramagnetic resonance in human fingernails: the sponge model implication. Radiat Environ Biophys. 2008; 47:515–526. [PubMed: 18584193]

Romanyukha A, Trompier F, LeBlanc B, Calas C, Clairand I, Mitchell CA, Smirniotopoulos G, Swartz HM. EPR dosimetry in chemically treated fingernails. Radiat Meas. 2007; 42:1110–1113. [PubMed: 18163159]

Romanyukha A, Reyes RA, Trompier F, Benevides LA. Fingernail dosimetry: current status and perspectives. Health Phys J. this issue.

Sevilla MD, D'Arcy JB, Morehouse KM. An electron spin resonance study of γ-irradiated frozen aqueous solutions containing dipeptides. Mechanisms of radical reaction. J Phys Chem. 1979; 83:2887–2892.

Snipes W, Horan PK. Electron spin resonance studies of free radical turnover in gamma-irradiated single crystals of alanine. Radiat Res. 1967; 30:307–315. [PubMed: 4289701]

Symons MC, Chandra H, Wyatt JL. Electron paramagnetic resonance spectra of irradiated finger-nails: a possible measure of accidental exposure. Radiat Prot Dosim. 1995; 58:11–15.

Symons MCR. Electron movement through proteins and DNA. Free Rad Biol Med. 1997; 22:1271–1276. [PubMed: 9098101]

Trompier F, Kornak L, Calas C, Romanyukha A, LeBlanc B, Mitchell CA, Swartz HM, Clairand I. Protocol for emergency EPR dosimetry in fingernails. Radiat Meas. 2007; 42:1085–1088. [PubMed: 18163158]

Wilcox DE, He X, Gui J, Ruuge AE, Li H, Williams BB, Swartz HM. Dosimetry based on EPR spectral analysis of fingernail clippings. Health Phys J. this issue.

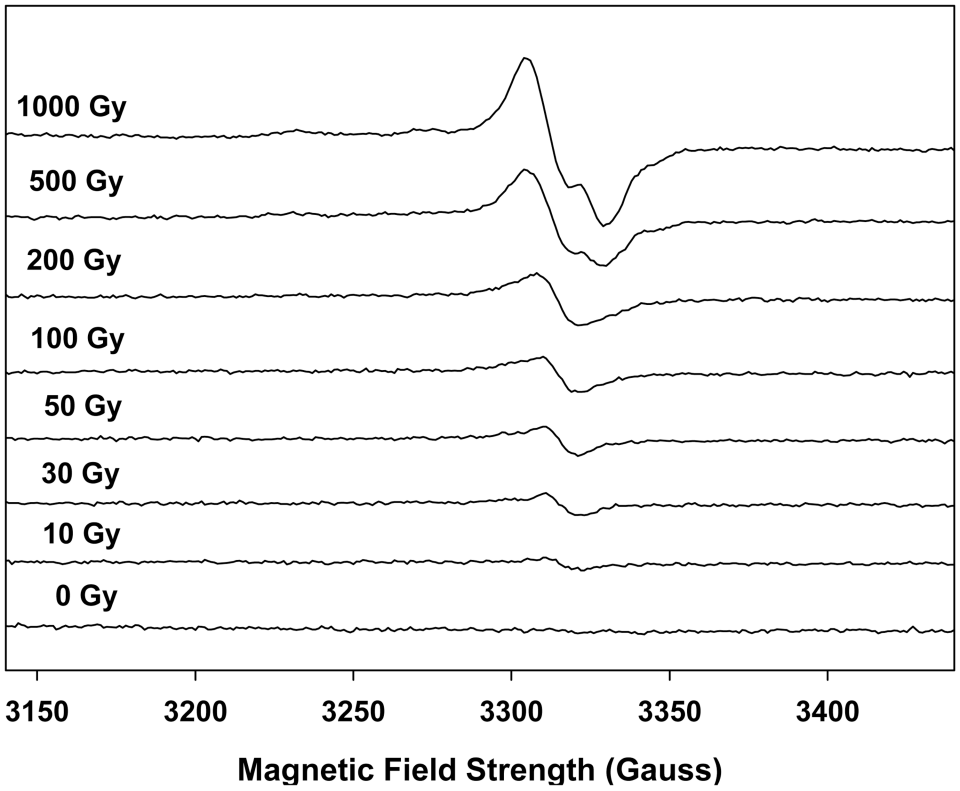

Figure 1.
Spectra from an x-ray irradiated single nail (8.9 mg) given additive doses of 0, 10, 30, 50, 100, 200, 500, and 1,000 Gy showing the qualitative changes in the spectra as a function of increasing dose. At a 10 Gy dose a singlet with a 10 G linewidth is the predominant feature. However as the dose increases beyond 10 Gy there are other, broader features that build into the spectrum.

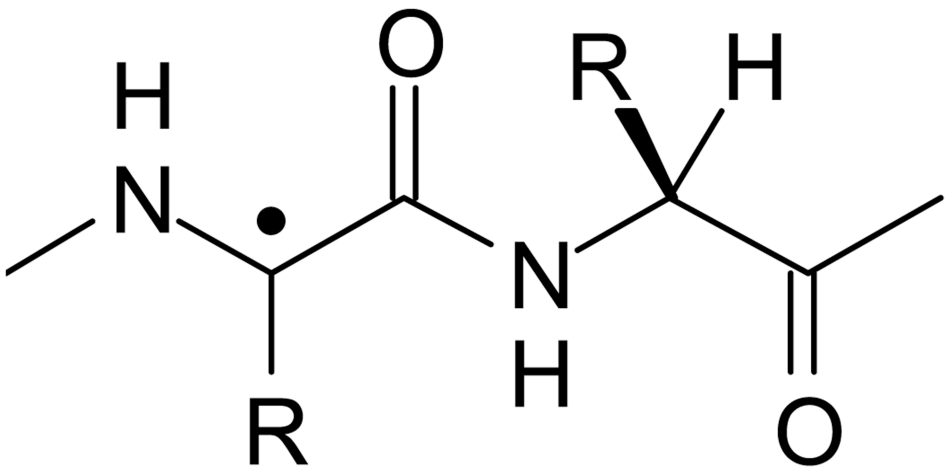

Figure 2.

Qualitative changes in the MIS spectra as a function of time and humidity in the same sample. The analysis was conducted on 6 nails (same volunteer) cut into 2×2 mm pieces (46 mg) to maximize the MIS signal for the purposes of spectral deconvolution analysis. The spectrum A was taken within 20 min of the sample preparation under ambient temperature (294-296 K) and humidity (55%). Spectra B, C and D were obtained after 4, 12 and 24 hr, respectively, of exposure to 72% relative humidity. The spectral trace at the bottom of the figure is from Fremy salt which is used as a field reference (g = 2.0056, aN = 13.09 G).

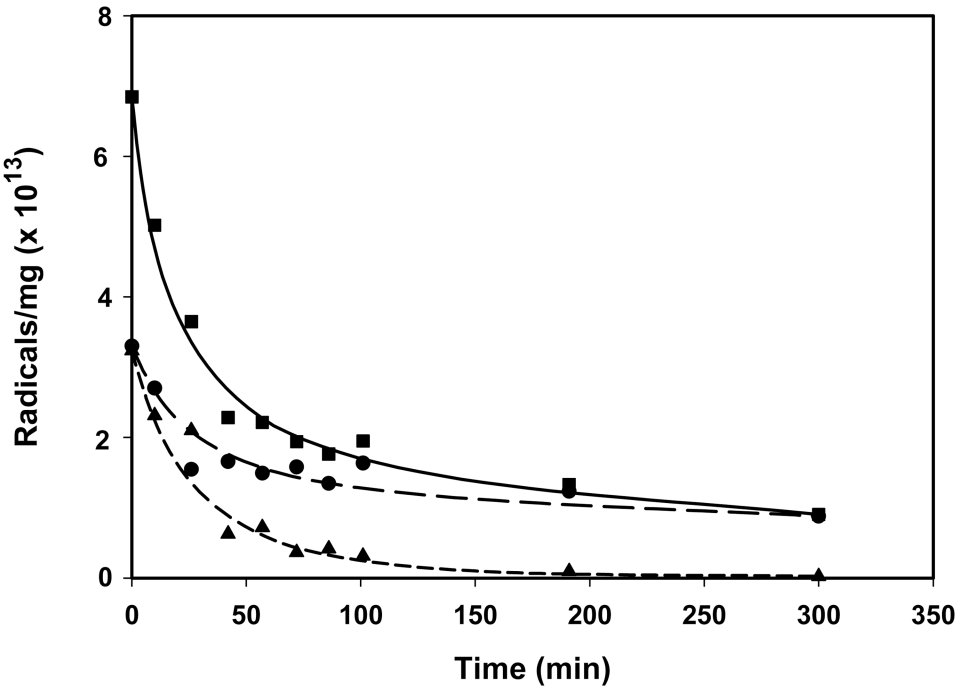

Figure 3.
RIS spectrum from a single nail clipping (8.9 mg) x-ray irradiated to 1,000 Gy (Spectrum A). The basis spectrum (B) for the singlet was subtracted from spectrum A, resulting in the doublet shown in spectrum C.

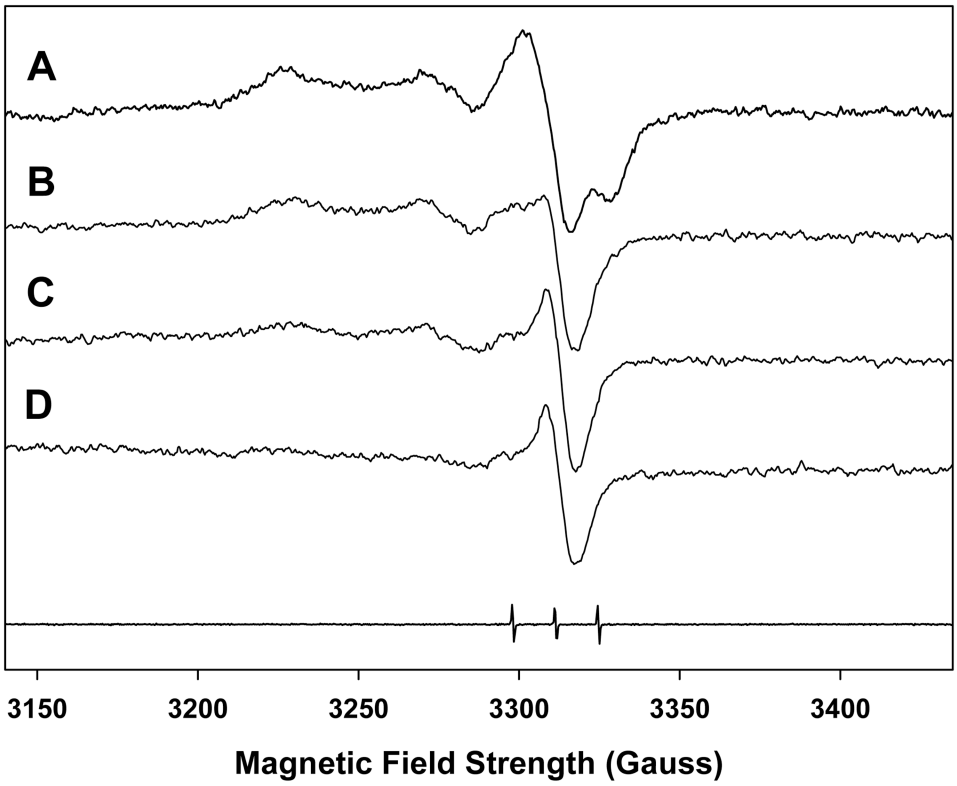

Figure 4.
MIS spectrum from 6 nails (same volunteer) cut into 2×2 mm pieces (46 mg) to maximize the MIS signal for the purposes of spectral deconvolution analysis. The basis spectrum (B) for the singlet was subtracted from spectrum A, resulting in the doublet shown in spectrum C.

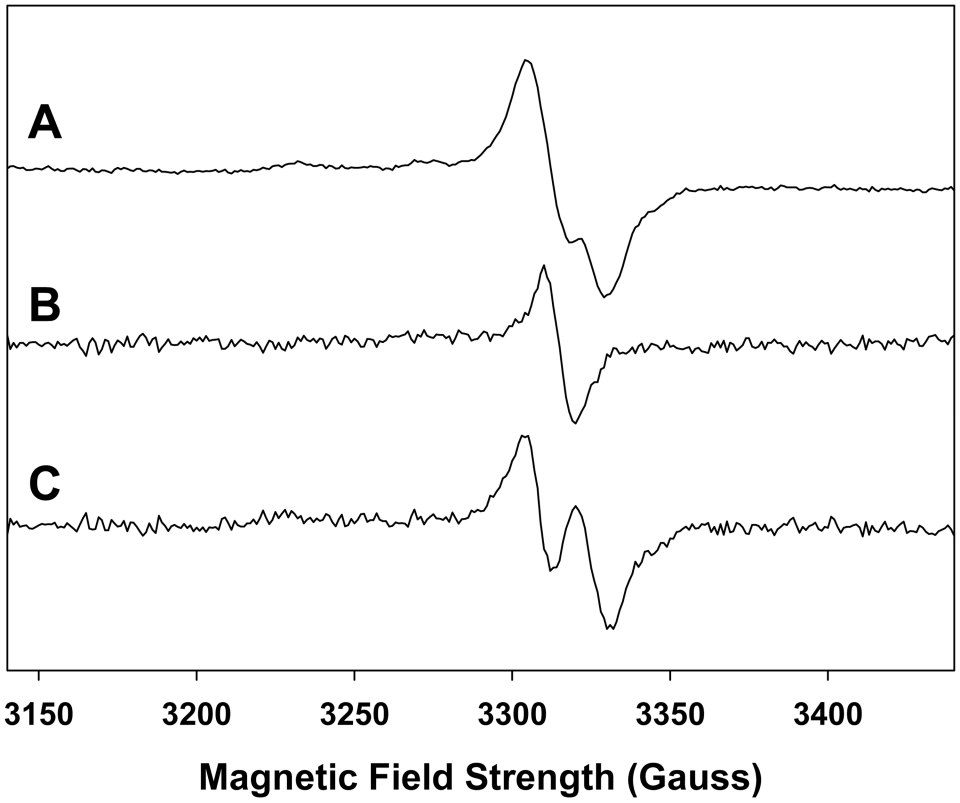

Figure 5.
Decay in the RIS signal in nails gamma-irradiated to 10 Gy as a function of contact time in water at 296 K. The points represent the mean peak-to-peak intensity ratios for the spectral line at g = 2.005 in clippings at each time point (RIS_X)relative to the initial intensity (RIS_0) post-radiation. Each time point represents a separate nail clipping obtained from the same individual and matched for mass (10 mg ± 1 mg). The error bars represent the standard deviation in the intensity ratios between five individuals. The nails were presoaked in water for 10 min, followed by 20 air dry before receiving the 10 Gy dose to remove the MIS.

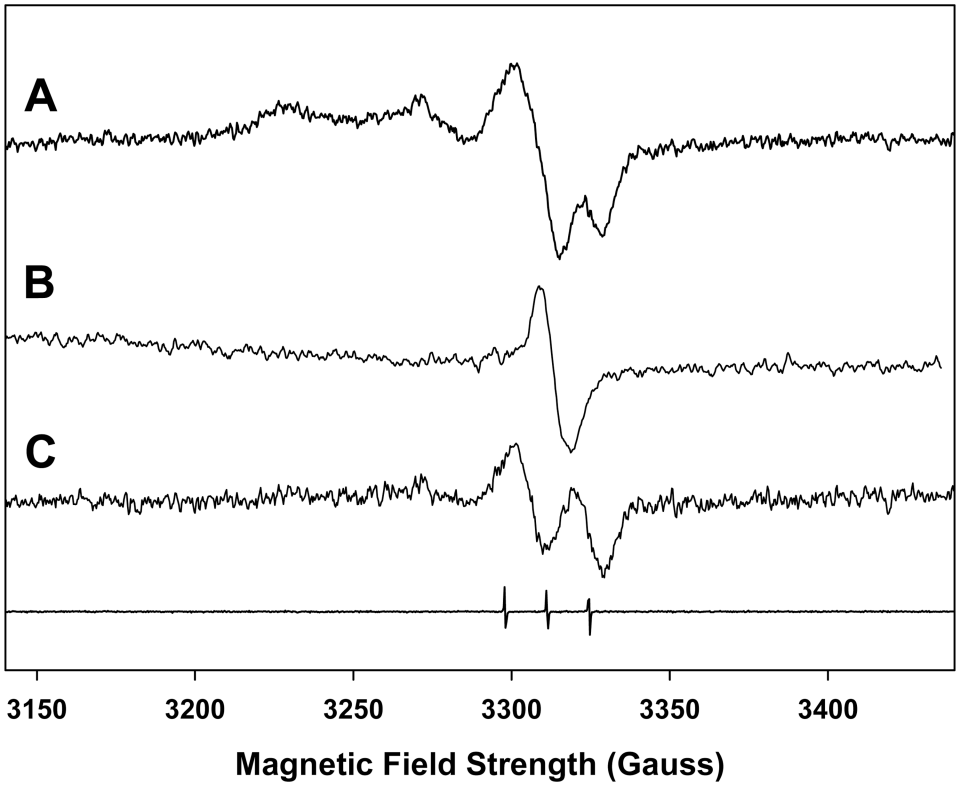

Figure 6.
Structural representations of a perthiyl (A) and sulfuranyl (B) radical. Either radical structural assignment would give rise to an anisotropic EPR spectrum with g-values at 2.056, 2.021, and 1.999, consistent with the downfield line positions seen in the high dose RIS and the MIS spectra in Figs. 4 and 5.

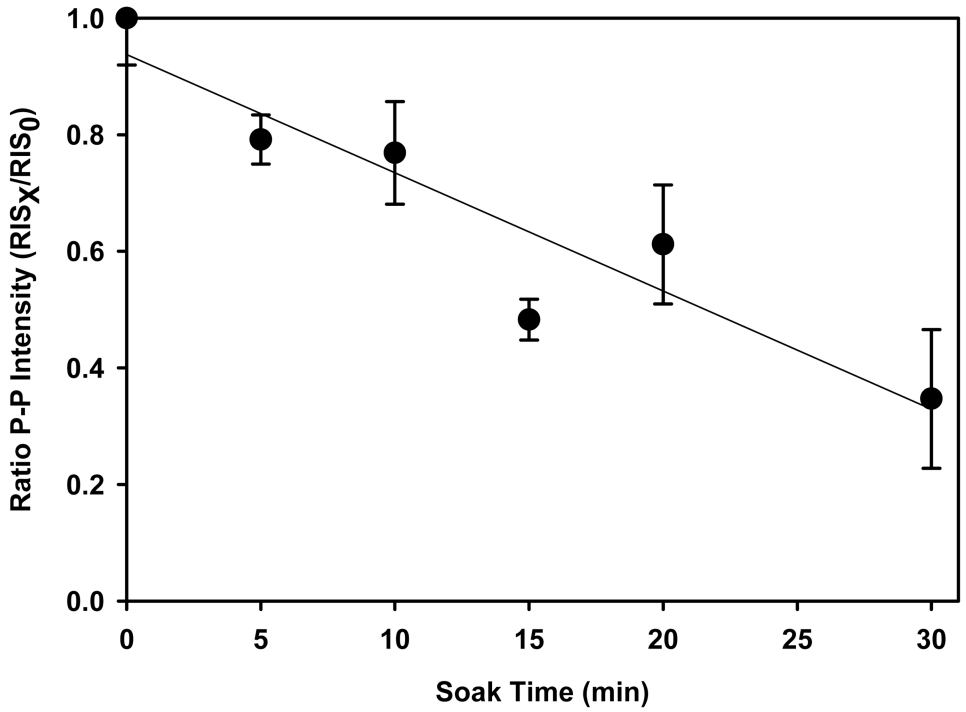

Figure 7.

Dose response curves for a finger nail (8.9 mg) given x-ray doses from 10 to 1,000 Gy. Spectra for each data point were taken within 10 min of the cessation of the radiation dose. The number of spins in the irradiated nail were determined against a $CuCl_2 \cdot 2H_2O$ standard (1.27×10^{17} spins). The r^2 value of the exponential fit to the data was 0.9977. The chemical yield calculated from this data for the total spectrum (square) is 403 nmol J^{-1}. The total spectra for each of the dose points was deconvoluted into the singlet and doublet spectra (i.e. as is shown in Fig. 4). From these deconvolutions, separate plots of the dose response behavior for the singlet (circle) and double (triangle) were obtained, with chemical yields of 327 and 122 nmol J^{-1} calculated for the singlet and doublet, respectively.

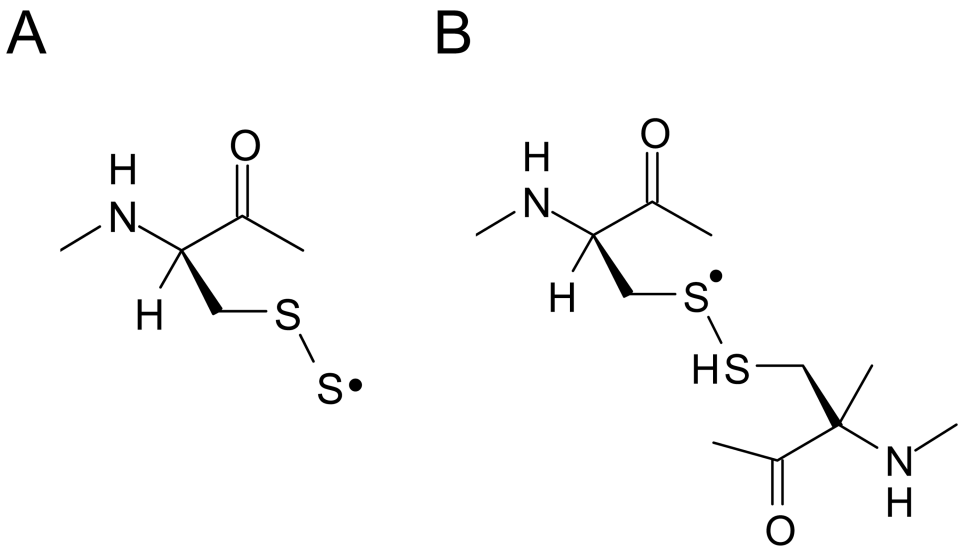

Figure 8.
Chemical yields calculated from the six different dose response studies performed on x-ray irradiated nail clippings from six volunteers. The error bars represent the standard error of the estimate. Nail masses used in these studies are as follows: Vol. 1 (8.9 mg), Vol. 10 (10.2 mg), Vol 12 (12.0 mg), Vol. 13 (10.4 mg), Vol. 14 (10.1 mg) and Vol. 15 (10.1 mg).

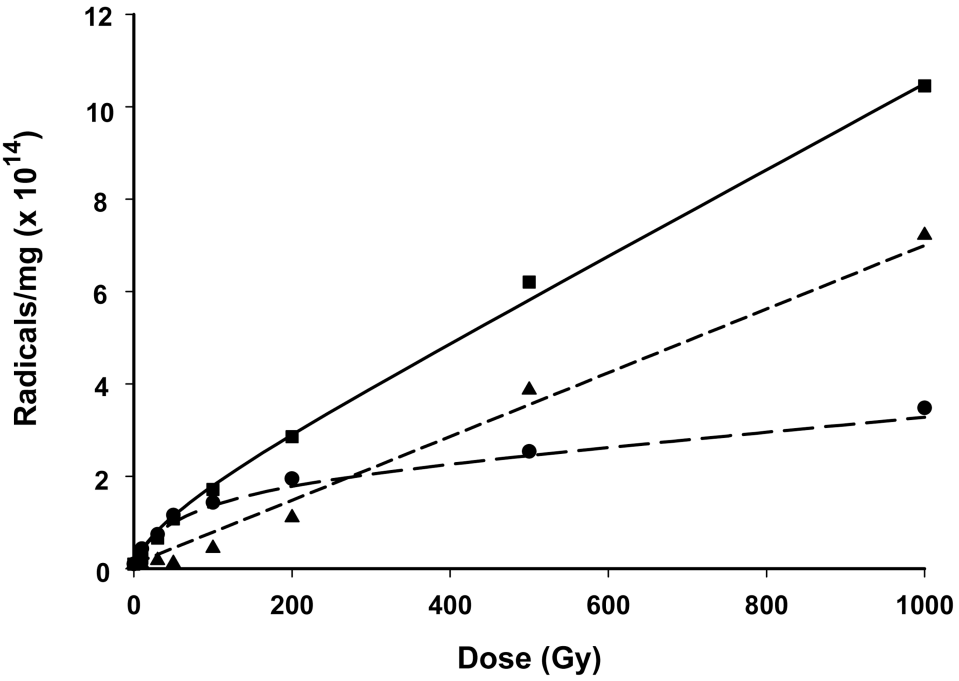

Figure 9.

Power saturation of the singlet at g = 2.0053 in RIS (A) and MIS (B) spectra. The data is plotted as the peak-to-peak (g = 2.0053) as a function of the square-root of the incident microwave power. The RIS spectrum was obtained from a nail (10 mg) x-ray irradiated to 100 Gy and then exposed to 74% relative humidity for 2 hr to remove the underlying doublet signal. The MIS spectrum was obtained from 10 2×2 nail clippings (same volunteer) that were exposed to 74% relative humidity for 12 hr to remove the underlying doublet and sulfuranyl radical signals.

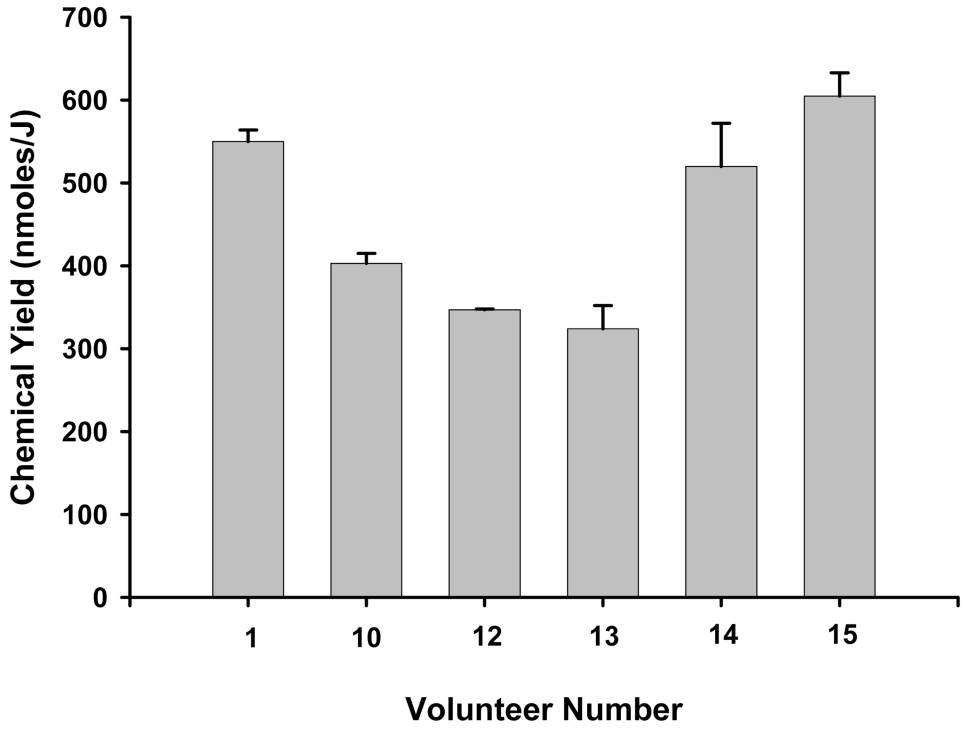

Figure 10.
Structural representation of an alpha-carbon radical on the peptide backbone.

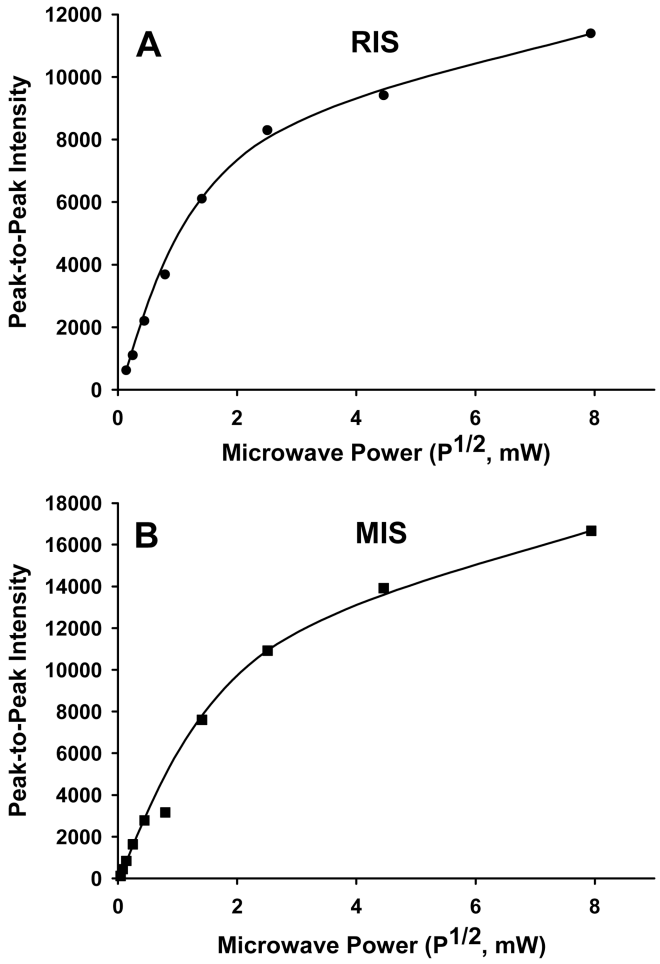

Figure 11.

Decay in the RIS signal in a single nail (8.9 mg) exposed to a humidity of 72% following a 1,000 Gy dose of x-ray radiation. The points represent the double integrals of the central singlet of the spectra taken at time points from 10 – 300 min post-irradiation. The number of spins in each time point spectrum was determined in reference to a $CuCl_2 \cdot 2H_2O$ standard. The data for the total spectrum (square) was fit to a two-phase exponential decay model. The r^2 value for this particular fit was 0.987. For each time point, spectral deconvolutions were conducted to extract the singlet and doublet signals. These data are plotted for the singlet (circle) and doublet (triangle) in the figure and fit to a one-phase exponential model.